

## Effect of Thermal Treatment of the $\text{Al}_2\text{O}_3$ and $\text{TiO}_2$ Supports on Properties of Dispersed Chromium Oxide in Oxidative Dehydrogenation of Isobutane

by B. Grzybowska, K. Samson, L. Keromnes\*, K. Wcisło,  
R. Dula and E.M. Serwicka

*Institute of Catalysis and Surface Chemistry, Polish Academy of Sciences,  
ul. Niezapominajek, 30-239 Kraków, Poland*

*(Received August 31st, 2000)*

Chromium oxide has been dispersed on  $\text{Al}_2\text{O}_3$  and  $\text{TiO}_2$  supports, heated between 500–1200°C, and the catalysts obtained have been tested in oxidative dehydrogenation of isobutane at 280°C. For the  $\text{CrO}_x/\text{Al}_2\text{O}_3$  system the thermal treatment of alumina, which leads to the decrease in the specific surface area and polymorphic transformations of the initial  $\gamma\text{-Al}_2\text{O}_3$  into  $\theta$ ,  $\Delta$  and  $\alpha$  modifications, does not affect the catalytic performance of the catalysts in the reaction under study. On the other hand, the transformation of anatase- $\text{TiO}_2$  into rutile- $\text{TiO}_2$ , occurring on heating at 1000°C, leads to catalysts of a higher activity and selectivity to isobutene. Amelioration of the catalytic properties for  $\text{CrO}_x/\text{rutile-TiO}_2$ , as compared with  $\text{CrO}_x/\text{anatase-TiO}_2$  catalysts, has been ascribed to changes in the structure of the  $\text{CrO}_x$  active centres, evidenced by ESR.

**Key words:** supported chromium oxide catalysts, alumina supported chromium oxide, titania supported chromium oxide, oxidative dehydrogenation of isobutane

Oxidative dehydrogenation, (ODH) of lower alkanes  $\text{C}_2\text{-C}_4$  has attracted in recent years much interest as a cheap way to obtain olefins for polymerization and oxidation [1–4]. The advantages of ODH over classical dehydrogenation (DH) (used commonly at present to produce olefins on industrial scale) lie in the lower reaction temperatures, due to the exothermicity of the oxidation reactions and in the absence of coke. The formation of the latter during DH results in fast deactivation of the catalysts, requiring their periodic regeneration in air.

Most of the works on ODH reactions have been concerned with propane and n-butane [1–4, 5]. Much less effort has been made to ODH of isobutane, in spite of the importance of its product-isobutene- a key reactant for production of methyl tertiary butyl ether (an additive to Pb-free petrol) and methacrylates. Few systems, reported so far as promising catalysts for this reaction, include the  $\text{ZnO-TiO}_2$  system [6], the metal pyrrophosphates (particularly  $\text{NiP}_2\text{O}_7$ ) [7], the  $\text{V}_2\text{O}_5\text{-MgO}$  catalysts [8] and Dawson-type heteropolycompounds containing tungsten [9]. All these systems were active at temperatures above 400°C.

---

\* Present address: Laboratoire d'Applications Plastiques, Elf Atochem S.A. – Usine de Saint Auban, 04600 Saint Auban, France.

Recently we have found that chromium oxide on oxide supports is active and selective in ODH of isobutane already at 200–300°C [10–15]. Chromium oxide, supported on lanthanum carbonate, has been also found active and selective in this reaction at low temperature [16]. The catalytic performance has been found to depend on the nature of the support [10]: the best results (selectivity to isobutene of about 50% at 10% conversion of isobutane), comparable with those given in literature, have been obtained for  $\text{CrO}_x/\text{Al}_2\text{O}_3$  [10–12],  $\text{CrO}_x/\text{TiO}_2$  [10,13] and  $\text{CrO}_x/\text{CeO}_2$  [14,15] systems.

The optimal amount of chromium oxide, deposited on the  $\text{Al}_2\text{O}_3$  and  $\text{TiO}_2$  supports, was found to be about 1 theoretical monolayer, mnl of  $\text{Cr}_2\text{O}_3$  [11,13], estimated from the crystallographic data of the oxide as equivalent to 10 at Cr per  $1 \text{ nm}^2$  of the support surface. Physicochemical characterization of the catalysts at this chromium content has shown the existence of the hexavalent chromium ions (about 25% of the total Cr content), present on the support surface in the form of polychromates, in addition to  $\text{Cr}^{3+}\text{O}_x$  species [11,13]. No optimization of the support structure, however, has been performed, commercial  $\gamma\text{-Al}_2\text{O}_3$  (Merck, basic), and  $\text{TiO}_2$  (anatase, Tioxide and Police, Poland) as received being used in the studies.

The present work is concerned with the effect of the thermal treatment of the  $\gamma\text{-Al}_2\text{O}_3$  and  $\text{TiO}_2$  supports on the catalytic performance of chromium oxide, deposited on their surface in the ODH of isobutane. The aim of the studies is to check to what extent the changes in the specific surface area of the supports, accompanying dehydroxylation of the surface [17] and their polymorphic transformations, which may occur during the heat treatment, modify the catalytic properties of the dispersed chromium oxide in this reaction. The effect of the type of a support, even of the same chemical nature, on properties of the active phase deposited on the support surface is generally recognized, though rarely studied systematically. In the selective oxidation on oxide systems much effort has been made to compare the structure and properties of vanadia phase, dispersed on different polymorphic modifications (anatase or rutile) of titania [18]. No data are, however, available concerning the effect of the titania or alumina structure on the properties of the deposited chromium oxide in selective oxidation reactions.

## EXPERIMENTAL

**Supports:**  $\gamma\text{-Al}_2\text{O}_3$  (Merck, basic, grain size 600–100 m), of specific surface area,  $S_{\text{sp}}$  equal  $111 \text{ m}^2/\text{g}$  was calcined for 5 h in a stream of air at 500, 900 and  $1200^\circ\text{C}$ .  $\text{TiO}_2$ -anatase (Tioxide, batch 93/204  $S_{\text{sp}} = 48 \text{ m}^2/\text{g}$ ) was subjected to the similar treatment at 500, 750 and  $1000^\circ\text{C}$ . The heating temperature was selected bearing in mind the thermal stability of various polymorphic forms of the two oxides [19–21]. Additionally  $\text{TiO}_2$ -rutile support (Police, Poland,  $S_{\text{sp}} = 7.5 \text{ m}^2/\text{g}$ ), denoted further in the text as TiRtPL, was used as received. The analysis of the original supports with the XPS technique has revealed the presence of the Si and Na impurities on the surface of  $\text{Al}_2\text{O}_3$  with the Si/Al ratio equal 0.06 and Na/Al = 0.01. The S impurity (S/Al = 0.02), due to the presence of sulphates, was found on the surface of the  $\text{TiO}_2$ -Tioxide: it disappeared after the calcination at  $900^\circ\text{C}$ . The TiRtPL support contained traces of the K and P impurities.

**Preparation of the catalysts:** The catalysts were obtained by impregnation of the supports, treated at various temperatures with appropriate amounts of aqueous solution of chromium nitrate,  $\text{Cr}(\text{NO}_3)_3 \cdot 9\text{H}_2\text{O}$ , (p.a. POCh, Gliwice, Poland), and evaporation followed by drying for 5 h at  $120^\circ\text{C}$  and calcination in a stream of air for 5 h at  $500^\circ\text{C}$ . For each catalyst the chromium content corresponded to 1 theoretical monolayer of  $\text{Cr}_2\text{O}_3$  (10 at Cr per  $1\text{ nm}^2$  of the support surface). The samples are denoted further in the text by symbols CrAl X and CrTi X, respectively for chromium oxide on alumina and titania, where X is the temperature of the heat treatment of the support. CrTiRtPL denotes the sample with the rutile TiRtPL support.

**Characterization of the catalysts:** Specific surface areas of the supports and catalysts,  $S_{\text{sp}}$ , were determined volumetrically by BET method using argon or krypton (for  $S_{\text{sp}} < 20\text{ m}^2/\text{g}$ ) as adsorbates. The samples were analyzed for the content of Cr ions in the oxidation state higher than  $3+$  with the Bunsen-Rupp (BR) method, described in [22]. The method consists in treating a sample with concentrated HCl, which leads to reduction of the higher valency chromium ions to  $\text{Cr}^{3+}$  and determination of the chlorine evolved by iodometric titration. XRD technique was used to determine the phase composition of the supports and catalysts. XR diffractograms were recorded with a Siemens D 5005 apparatus and compared with the ASTM data. ESR spectroscopy was used for some catalysts to determine the state of the  $\text{Cr}^{3+}$  ions. The ESR spectra were recorded at room and at liquid nitrogen temperatures with an X-band SE/X spectrometer (Technical University, Wrocław). Diphenylpicrylhydrazyl (DPPH) and NMR field marker were used to determine the g-factors.

**Catalytic tests:** The activity of the catalysts in the ODH of isobutane was measured in a fixed-bed flow apparatus at  $280^\circ\text{C}$  with on-line gas chromatography analysis of the substrates and products. Different conversions were obtained by varying the contact time from 0.2 to 2 s: the latter was effectuated by changing the flow rate of the reaction mixture. A stainless steel reactor (120-mm long, ID 13 mm) was coupled directly to a series of gas chromatographs. Isobutene and carbon dioxide were found to be the main reaction products. Small amounts of carbon monoxide (about 5% of the total amount of the products) were also observed. The amounts of the degradation products ( $\text{C}_2$ ,  $\text{C}_3$ ) and of oxygenates were below 1% of the products. The carbon balance, calculated taking into account isobutene, CO and  $\text{CO}_2$ , was  $97 \pm 2\%$  for conversion  $\geq 10\%$ , at lower conversion the C balance was poorer ( $90 \pm 5\%$ ). The reaction mixtures contained 9.2 vol. -% of isobutane (Phillips Petroleum Corp., 99%) in air. One half millilitre of a catalyst sample (about 0.5 g, grain size 0.63–1 mm), diluted (1:1) with the glass beads of the same diameter was used. It has been checked in preliminary measurements, in which the mass and the grain size of a sample were varied that, under these conditions, the transport phenomena do not limit the reaction rate. The total conversion of isobutane did not exceed 20%.

The catalytic data are presented in the form of plots of the selectivity to isobutene  $S_i$  versus the total conversion of isobutane C.  $C = N_0 - N_f / N_i \times 100$ ,  $S_i = N_i / \Sigma N \times 100$ , where  $N_0$  and  $N_f$  are the concentrations of isobutane at the entrance and the exit of the reactor respectively,  $N_i$  is a concentration of isobutene in the exit gas,  $\Sigma N = N_i + 1/3N_{\text{CO}_2} + 1/3N_{\text{CO}}$ . For a given sample the values of C and S were reproducible within 2–5%. The initial total rates of the isobutane disappearance per unit of the catalyst surface,  $V_{\text{sp}}$ , were also calculated by extrapolating the conversion data to 0-th contact time. A blank test without a catalyst or with glass beads in the reactor showed no conversion of alkanes at the reaction temperature. Pure alumina and titania supports were not active either, the isobutane conversion at  $280^\circ\text{C}$  being lower than 0.2%. No deactivation of the catalysts was observed during 10 h of the measurement.

## RESULTS AND DISCUSSION

Table 1 presents the results of characterization of the supports and catalysts. For both supports the specific surface area,  $S_{\text{sp}}$  decreases with the increase in the temperature of the heat treatment: the changes of  $S_{\text{sp}}$  are particularly drastic for the supports calcined at temperatures equal or higher than  $1000^\circ\text{C}$ . Such behaviour is commonly observed for oxides and ascribed to the loss of the surface OH groups, which favours the sintering of the oxide [17]. The XRD analysis has shown the changes in the phase composition, induced by the heating of the supports. In the case of  $\text{Al}_2\text{O}_3$  the original

sample containing  $\gamma$ -alumina is transformed into a mixture of polymorphs  $\gamma+\theta+\alpha$  ( $\gamma$  modification being a predominant phase) after heating at 500°C, a mixture of  $\Delta$  (predominant) and  $\alpha$  is found after heating at 900°C and pure  $\alpha$ -Al<sub>2</sub>O<sub>3</sub> at 1200°C. For TiO<sub>2</sub>, heating at 1000°C causes the transformation of anatase into the rutile form of titania. The XR diffractograms of the catalysts showed only the patterns of the supports. No lines characteristic of chromium oxides have been observed, which indicates a good dispersion of the chromium oxide phase on the support surface. The specific surface areas of the catalysts do not vary considerably from those of pure supports. Slight decrease with respect to the supports, observed for both alumina and titania calcined at 500°C (of the highest  $S_{sp}$ ) can be due to partial blocking of the support pores with the chromium oxide phase. No clear tendency in the changes of  $S_{sp}$  is seen for the catalysts deposited on the supports calcined at higher temperatures. The fraction of Cr ions of the valency higher than +3 is practically constant for the CrAl catalysts, which suggests that the chromium oxide dispersed in the form of polychromates has a similar structure, irrespectively of the calcination temperature of the support. In the case of the CrTi catalysts, the fraction of the Cr<sup>6+</sup> ions is considerably higher for the catalyst containing low specific area rutile as a support and only slightly higher for the TiRtPL support of the higher specific surface area.

**Table 1.** Characteristics of supports and catalysts.

CrO <sub>x</sub> /Al <sub>2</sub> O <sub>3</sub>						
Catalyst	Support calcn. temp. [°C]	$S_{sp}$ support [m <sup>2</sup> /g]	XRD support	Wt % Cr	$S_{sp}$ catalyst [m <sup>2</sup> /g]	Cr <sup>+6</sup> [at/nm <sup>2</sup> ]
CrAl 500	500	111.4	$\gamma^*+\theta+\alpha$	8.7	102.7	2.6
CrAl 900	900	61.8	$\Delta^*+\alpha$	5.1	64.6	2.7
CrAl 1200	1200	5.6	$\alpha$	0.5	6.4	2.7

\* predominant phase.

CrO <sub>x</sub> /TiO <sub>2</sub>						
Catalyst	Support calcn. temp. [°C]	$S_{sp}$ support [m <sup>2</sup> /g]	XRD support	Wt % Cr	$S_{sp}$ catalyst [m <sup>2</sup> /g]	Cr <sup>+6</sup> [at/nm <sup>2</sup> ]
CrTi 500	500	49.7	anatase	4.1	42.7	1.9
CrTi 750	750	25.9	anatase	2.2	20.5	1.5
CrTi 1000	1000	1.0	rutile	0.09	1.0	4.6
CrTiRtPL	–	7.5	rutile (10% anatase)	0.6	7.0	2.2

Figs 1 and 2 present the plots of the selectivity to isobutene as a function of the total isobutane conversion at 280°C for the CrAl and CrTi catalysts respectively. Table 2

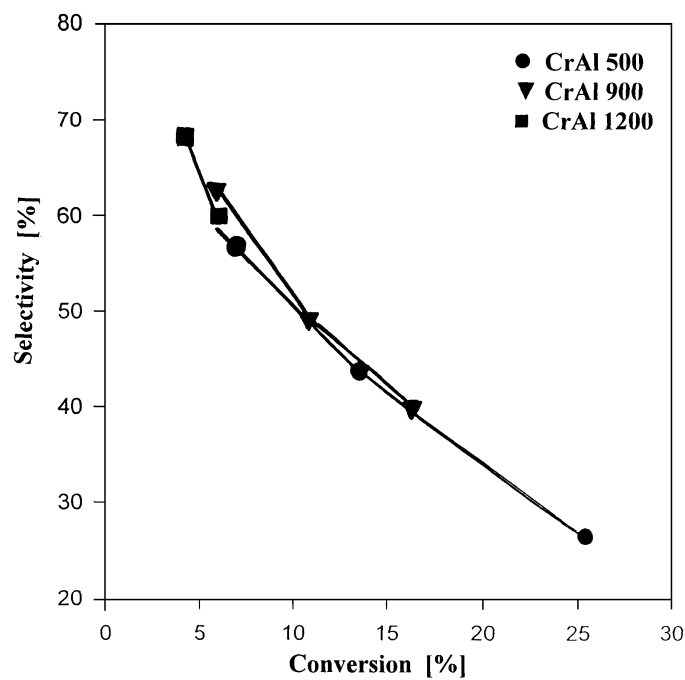


**Figure 1.** Selectivity to isobutene as a function of the total isobutane conversion at 280°C for CrO<sub>x</sub>/Al<sub>2</sub>O<sub>3</sub> catalysts.

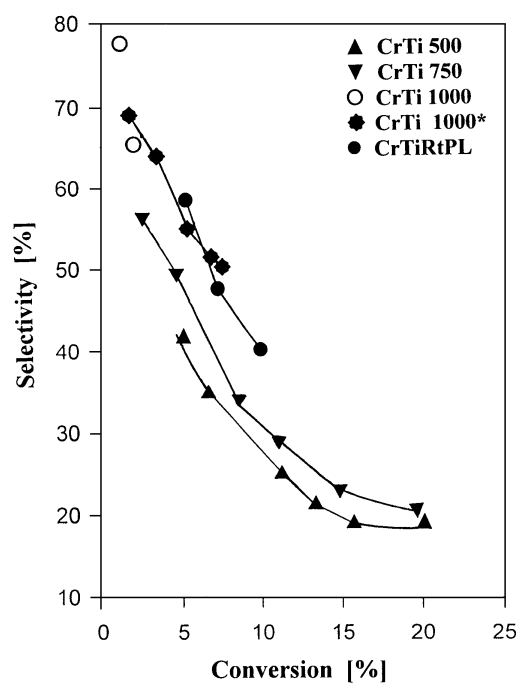


**Figure 2.** Selectivity to isobutene as a function of the total isobutane conversion at 280°C for CrO<sub>x</sub>/TiO<sub>2</sub> catalysts.\* : catalytic test at 370°C.

gives the values of the initial specific rate of the isobutane consumption at 280°C,  $V_{sp}$  and compares the selectivities to isobutene at the same conversion of isobutane (6%),  $S_{i6}$  for the studied samples. For both series of the catalysts, the selectivity to isobutene decreases with the increasing conversion, which is accompanied by the equivalent increase in the selectivity to carbon oxides. This confirms the consecutive reaction pathway, commonly observed for the ODH reactions of alkanes [1–5], and found previously for the isobutane ODH on supported chromium oxide catalysts [11–13].

**Table 2.** Initial specific rate,  $V_{sp}$  and selectivity to isobutene at 6% conversion,  $S_{i6}$  for oxidative dehydrogenation of isobutane at 280°C on  $Al_2O_3$  – and  $TiO_2$  – supported chromium oxide catalysts.

CrO <sub>x</sub> /Al <sub>2</sub> O <sub>3</sub> catalysts		
Catalyst	$V_{sp} \times 10^{-8}$ [mol/s m <sup>2</sup> ]	$S_{i6}$ [%]
CrAl 500	1.1	60
CrAl 900	1.5	62
CrAl 1200	1.6	60

CrO <sub>x</sub> /TiO <sub>2</sub> catalysts		
Catalyst	$V_{sp} \times 10^{-8}$ [mol/s m <sup>2</sup> ]	$S_6$ [%]
CrTi 500	0.7	35
CrTi 750	0.9	42
CrTi 1000	2.2	nm
CrTiRtPL	1.8	53

nm – not measured.

Isobutene, formed in the first step of the reaction, is oxidized further to carbon oxides. In the case of the CrAl system the points corresponding to different catalysts are located on practically the same curve and the selectivities to isobutene at comparable conversions have very close values. Moreover, the values of the initial specific rate of the isobutane consumption are very close. These results indicate that the catalytic properties in the ODH of isobutane of the chromium oxide phase deposited on alumina are not influenced by the type of the polymorphic modification of this oxide, or by the specific surface area of the support. In contrast, the properties of the CrTi catalysts depend on whether the chromium oxide phase is deposited on the anatase or rutile modification of titania. For the samples CrTi 500 and CrTi 750, containing the anatase form of  $TiO_2$ , but differing by their specific surface area, the selectivities at comparable conversions and the values of the specific rates do not differ markedly. For the CrTi 1000 sample, the value of the initial specific rate is significantly higher than that for the anatase-based samples. The selectivities to isobutene appear to be

also higher, though owing to the very low specific surface area, only the data at low conversions ( $< 5\%$ ) were obtained at  $280^\circ\text{C}$ . The tests for the CrTi 1000 catalyst at  $370^\circ\text{C}$ , (at which higher conversions could be reached) have also shown higher selectivities to isobutene than those for the anatase-containing samples at  $280^\circ\text{C}$ , in spite of the fact that the selectivities to partial oxidation products in selective oxidation reactions usually decrease with the increase in the reaction temperature [23]. The catalytic tests for the CrTiRtPL sample of the higher  $S_{sp}$  at the same temperature as that used in the studies of the anatase-containing catalysts ( $280^\circ\text{C}$ ) confirm that, indeed, the initial rate of the reaction and selectivities to isobutene of the rutile-deposited chromium oxide catalysts are higher than those obtained for the anatase-supported ones. Different catalytic performance for the catalysts of these two types suggests that the active  $\text{CrO}_x$  species on anatase and rutile may have different structure. The low specific area of the rutile-based catalysts renders impossible the comparison of the structure of the dispersed chromium oxide phase by the vibrational spectroscopies. The very sensitive ESR technique has then been used for this purpose.

The ESR analysis of the chromium containing catalysts shows that the type of the support influences significantly the nature and relative quantities of various paramagnetic Cr species present in the solids. Figs. 3a and b show the spectra of CrTi 500 and CrTi 1000 samples respectively. In both cases the spectra are overlaps of at least two signals of various intensities. In both samples there is a broad, nearly symmetric line with  $g \cong 2.0$  and  $\Delta H_{p-p} \cong 800\text{G}$  for CrTi 500 and  $\Delta H_{p-p} \cong 600\text{G}$  for CrTi 1000. This signal dominates the spectrum of CrTi 500, while in the CrTi 1000 its intensity is lower. In the literature such signals are designated  $\beta$  and generally assigned to clustered Cr(III) species in pseudo-octahedral symmetry [24–28]. The temperature characteristics of the signals indicates that the nature of the clusters depends on the type of the carrier. In the rutile-based sample CrTi 1000 the  $\beta$ -signal disappears at liquid nitrogen temperature pointing to the existence of antiferromagnetic order within the clusters responsible for this absorption. In the anatase-supported catalyst CrTi 500 the  $\beta$ -signal is visible also at  $77\text{K}$ , which suggests that the clusters are of amorphous nature, lacking long range ordering. The other signal, present in the CrTi 500 catalyst, is a narrow, sharp line at  $g \cong 1.97$ . Signal of this type, observed also in other supported Cr-containing systems, has been assigned to Cr(V) species and is referred to as the  $\gamma$ -signal [24–29]. There is no such signal in the spectrum of CrTi 1000. Here, the signal superimposed on the  $\beta$ -component is composed of a set of narrow lines, forming a characteristic pattern typical of Cr(III) ions substituting for Ti(IV) in the rutile lattice [30,31]. It is worthwhile to mention that the low temperature spectrum of CrTi 500 displays an additional weak feature around  $g \cong 5.0$ . This may be taken as an indication that yet another Cr species exists on the surface of the support, namely dispersed Cr(III) ions in strongly distorted axial surrounding. Species of this type are known to produce ESR signal designated  $\delta$ , whose most characteristic feature is a positive lobe at  $4 < g < 5$  [24–28, 32].

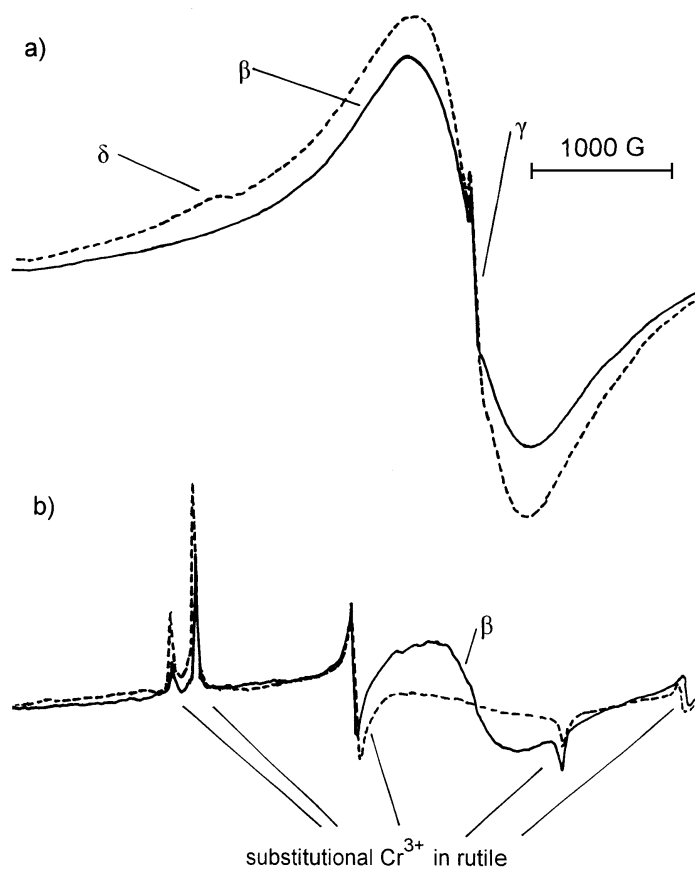


**Figure 3.** ESR spectra of  $\text{CrO}_x/\text{TiO}_2$  catalysts: a) CrTi 500, b) CrTi 1000.

The EPR data indicate then a different structure of chromium – containing centres in anatase- and rutile- supported catalysts. In addition to the change in structure of  $(\text{CrO}_x)_n$  clusters on the surface of the supports, chromium ions in the latter catalysts enter the rutile lattice forming the solid solution.

It cannot be decided at present, which of these modifications are responsible for the higher activity and selectivity to isobutene for rutile-supported chromium oxide, as compared with the anatase-supported catalysts. It can be only observed that the environment of  $\text{Cr}^{3+}$  ions in the rutile  $\text{TiO}_2$  is different than that in the  $(\text{CrO}_x)_n$  clusters on the surface of the supports. In view of the lower reducibility of  $\text{TiO}_2$ , as compared with that of chromium oxides, one may expect that the  $\text{Cr-O-Ti}$  bonds in the solid solution in the rutile matrix are stronger than the  $\text{Cr-O}$  bonds in the chains  $\text{Cr-O-Cr-O}$  of  $(\text{CrO}_x)_n$  clusters attached to the surface. The higher metal–oxygen bond energy in oxide catalysts has been correlated with a higher selectivity to selective oxidation products [33], which could account for the higher selectivity to isobutene on rutile – containing catalysts.



## CONCLUSIONS

1. Thermal treatment of the  $\gamma$ -Al<sub>2</sub>O<sub>3</sub> (Merck) and TiO<sub>2</sub> (Tioxide-anatase) leads to polymorphic transformations and to the decrease in specific surface area.  $\Delta$ -Al<sub>2</sub>O<sub>3</sub> with admixture of  $\alpha$  and pure  $\alpha$ -Al<sub>2</sub>O<sub>3</sub> are formed after calcination of  $\gamma$ -Al<sub>2</sub>O<sub>3</sub> at 900 and 1200°C respectively. The anatase-rutile transformation is observed after calcination of TiO<sub>2</sub> at 1000°C.
2. The catalytic properties in oxidative dehydrogenation of isobutane of catalysts, obtained by deposition of one theoretical monolayer of chromium oxide on the Al<sub>2</sub>O<sub>3</sub> support calcined at different temperatures, are independent of the specific surface area and of the type of polymorphic modification of Al<sub>2</sub>O<sub>3</sub>. For the similar chromium oxide/TiO<sub>2</sub> catalysts the total initial activity and selectivity to isobutene are higher for the rutile-supported as compared with the anatase-supported samples.
3. Better catalytic performance of the rutile-supported chromium oxide catalysts in oxidative dehydrogenation of isobutane is ascribed to a different structure of active CrO<sub>x</sub> centres as shown by the ESR technique: in addition to (Cr<sup>3+</sup>O<sub>x</sub>)<sub>n</sub> clusters of different structure than those on the anatase, the ESR analysis evidenced the presence of Cr<sup>3+</sup> ions in the rutile matrix.

## Acknowledgments

Laurent Keromnes acknowledges the support from Elf Aquitaine during his training stay in Poland.

## REFERENCES

1. Albonetti S., Cavani F. and Trifirò F., *Catal. Rev. -Sci. Eng.*, **38**(4), 413 (1996).
2. Cavani F. and Trifirò F., *Catal. Today*, **36**, 431 (1997).
3. Baerns M. and Buyevskaya O., *Catal. Today*, **45**, 13 (1998).
4. Kung H.H., *Adv. Catal.*, **40**, 1 (1994).
5. Mamedov E.A. and Cortés Corberán V., *Appl. Catal.*, **127**, 1 (1995).
6. Lysova N.N., Tmenov D.N. and Luk'yanenko P., *Russ. Zh. Prikl. Khim.*, **65**, 1848 (1992).
7. Takita Y., Kurosaki K., Mizuhara Y. and Tshihara T., *Chem. Lett.*, 335 (1993).
8. Michalakos P.M., Kung M.C., Jahan I. and Kung H.H., *J. Catal.*, **140**, 226 (1993).
9. Cavani F., Comuzzi C., Dolcetti G., Etienne E., Finke R. G., Sella G., Trifirò F. and Trovarelli A., *J. Catal.*, **160**, 317 (1996).
10. Grabowski R., Grzybowska B., Słoczyński J. and Wcisło K., *Appl. Catal. A*, **144**, 335 (1996).
11. Grzybowska B., Słoczyński J., Grabowski R., Wcisło K., Kozłowska A., Stoch J. and Zieliński J., *J. Catal.*, **178**, 687 (1998).
12. Słoczyński J., Grzybowska B., Grabowski R., Kozłowska A. and Wcisło K., *Phys. Chem. Chem. Phys.*, **1**, 333 (1999).
13. Grzybowska B., Słoczyński J., Grabowski R., Wcisło K., Kozłowska A., Stoch J. and Serwicka E., *Polish J. Chem.*, **72**, 2159 (1998).
14. Moriceau P., Grzybowska B., Barboux Y., Wrobel G. and Hecquet G., *Appl. Catal. A*, **168**, 269 (1998).
15. Moriceau P., Grzybowska B., Gengembre L. and Barboux Y., *Appl. Catal. A*, **199**, 73 (2000).
16. Hoang H., Mathews J. F. and Pratt K. C., *J. Catal.*, **171**, 320 (1997).
17. Boehm H.P., *Adv. Catal.*, **16**, 179 (1966).
18. Grzybowska-Świerkosz B., *Appl. Catal. A*, **157**, 263 (1997).

19. Knözinger H. and Ratnasamy P., *Catal. Rev.-Sci. Eng.*, **17(1)**, 31 (1978).
20. Lida Y. and Ozaki S., *J. Am. Ceram. Soc.*, **44(3)**, 120 (1961).
21. Shannon R.D. and Pask J.A., *J. Am. Ceram. Soc.*, **48(8)**, 391 (1965).
22. Dereń J., Haber J. and Słoczyński J., *Chem. Anal.*, **6**, 659 (1961).
23. Bielański A. and Haber J., "Oxygen in Catalysis" (Dekker, NY, 1991).
24. O'Reilly D.E. and Mc Iver D.S., *J. Phys. Chem.*, **6**, 276 (1962).
25. Poole C.P. and Mac Iver D.S., *Adv. Catalysis*, **17**, 224 (1967).
26. Cimino A., Cirdischi D., De Rossi S., Ferraris G., Gazzoli D., Indovina V., Occhiuzzi M. and Valigi M., *J. Catal.*, **127**, 761 (1991).
27. Weckhuysen B.M., De Ridder L.M., Grobet P.J. and Schoonheydt R., *J. Phys. Chem.*, **99**, 320 (1995).
28. Weckhuysen B.M., Schoonheydt R.A., Mabbs F.E. and Collison D., *J. Chem. Soc. Farad. Trans.*, **92**, 2431 (1996).
29. Cordischi D., Campa M. C., Indovina V. and Occhiuzzi M., *J. Chem. Soc. Farad. Trans.*, **90**, 207 (1994).
30. Evans J.C., Relf C.P., Rowlands C.C., Egerton T.A. and Pearman A.J., *J. Mater. Sci. Lett.*, **3**, 695 (1984).
31. Köhler K., Schläpfer C.W., von Zalewsky A., Nickl J., Engweiler J. and Baiker A., *J. Catal.*, **143**, 201 (1993).
32. Doeuff S., Henry M., Sanchez C. and Livage J., *J. Non-Cryst. Solids*, **89**, 84 (1987).
33. Grzybowska-Świerkosz B., *Topics Catal.*, **11/12**, 23 (2000) and references therein.